INTERNATIONAL JOURNAL OF
COASTAL & OFFSHORE ENGINEERING
IJCOE Vol.3/No. 1/Spring 2018 (21-34)

Available online at: http://ijcoe.org/browse.php?a_code=A-10-180-1&sid=1&slc_lang=en

A Comprehensive Study of an Identical Submarine Subjected to Explosion

Rouhollah Amirabadi[1*], Reza Ghazangian[2]

[1*] *Assistant Professor of Civil Engineering, University of Qom; r.amirabadi@qom.ac.ir*
[2] *PhD of Civil Engineering, University of Qom; gharangian@gmail.com*

ARTICLE INFO

Article History:
Received: 18 Apr. 2018
Accepted: 9 Jun. 2018

Keywords:
Finite Element Method
Doubly asymptotic approximation
Submarine
Explosion

ABSTRACT

Despite the enormous military threats against the country's military facilities, especially the naval industry, correct understanding of the behavior of these structures in efficacy of explosion, analysis and design of this industry has been much importance than ever before. An important class of these threats, is underwater explosion and its effect on various structures, Floating or submerged. In this paper, the researcher first introduces the underwater explosion phenomena and theories that govern the propagation of fluid hydrodynamics, shock waves from the explosion and its interaction with floating and also submerged structures have been investigated. Finally, numerical studies (FEM) of the behavior of a super submarine subject to underwater explosion have been provided by ABAQUS software and some results have been obtained such as: response with different frequencies, the place of radiation boundary in interaction of water and construction, the effect of added mass and hydrodynamic pressure.

1. Introduction

Naval structures have many applications, especially in the oil and gas industries of every nation. The design of these structures has been influenced by various factors such as wind, wave, current, earthquake, and dead and live loads. On the other hand, with the spread of military threats against the country, the analysis and design of these structures under the explosive loads become apparent. One of the crucial issues in the study of water-structure interaction is underwater explosions and their impact on submerged structures, as they are strategically critical in terms of engineering application and passive defense. Since World War II, this subject has been studied and underwater explosions have been used in many industrial projects such as the shaping of metal planes and military operations and recently for the removal of obsolete marine structures such as platforms. The waves caused by underwater explosions have a remarkable impact on submerged structures like submarines, pipelines, oil platforms and facilities etc. Therefore, the detailed analysis of underwater explosions has been considered a necessity in reducing the damage of these structures.

In engineering sciences, it is sometimes essential to dismantle all the devices into single components and parts with understandable behavior and then restore the device based on such components, in order to clearly understand the environmental behavior and its natural processes. Numerical methods are one of these processes, capable of modeling the behavior of complex phenomena by discretization. Moreover, two cases are often posed with regard to the dispersal of waves in any space. In the first case, we deal with waves of small amplitude and then in the second case, these are shockwaves and therefore we deal with the waves of finite amplitude. The waves which are created in the vicinity of the explosions, are of the second type.

In this article, we first express the theories of interaction analysis for water and submerged structures being subject to explosions and then we use ABAQUS software to provide a numerical modeling for a submarine.

2. Research history

Cole is the first scholar to explain the equations regarding underwater explosions in his research [1]. By describing various processes of explosions, he has developed a new way in this field. The complete analysis of the problem of underwater explosion involves solving the equation of structural vibration and the concurrent diffusion of waves from the explosion source through the fluid. The methods used to analyze this phenomenon are either the expansion of series or the use of variable changes. In 1999, Maire collected the reference problems which propose an analytical and precise solution to the water-structure interaction [2]. Since the introduction of all

these instances is beyond the scope of this article, it would sufficient to report a few cases in this regard.
Shock chamber: This model proposes a one-dimensional solution to the problem of shock and wave diffusion due to the interaction of two fluids in a stationary state in the Cartesian-Riemann system.
Rayleigh Model: A one-dimensional solution is proposed in the spherical structure for the dynamic incompressible fluids.
Primakoff Solution: A one-dimensional solution is provided in the spherical structure for the dispersal of shockwaves in the water caused by movable boundaries.
Table 1 summarizes these cases.

Table 1. General issues for continuous flow field

	Analytical\Empirical	Water	Bubbly\ Cavitating Water	Idealized Sediment	In-Suit Sediment	Air	Explosive
Shock Tube	A	●	○	○	○	○	○
Rayleigh-Plesset Solution	A	●	○	○	○	○	○
Primakoff Solution	A	●	○	○	○	○	○
Caviated Water Impact	A	○	●	○	○	○	○
P.alpha Shock Tube	A	○	○	●	○	○	○
Wardlaw/Mair Bubble	A	●	○	○	○	○	○
UNDEX Similitude	E	●	○	○	○	○	○
Spark-Generated Bubbles	E	●	○	○	○	○	○
SRI Spherical Sand Shock	E	○	○	●	○	○	○
Snay Goertner Bubble	E	●	○	○	○	○	○

The black and white circles indicate existence and absence respectively.
In 1984, Felippa and Deruntz developed a finite element method for cavitation based on the works that Newton had done between 1978 and 1981 on the impact of cavitation on the underwater explosion. In this method, the wave field inside the fluid was modeled based on a potential function of scalar displacement. CAFE elements were first used by its originators in CFA computer program. The fluid boundaries were considered based on the method used by Geers in 1978. These boundaries which are called doubly asymptotic approximation are actually a boundary element method that provides accurate answers at the initial and final intervals of the analysis. USA computer program developed by Deruntz in 1989 has been based on this method [3,4]. Then, in 1990, another program called USA/LS_DYNA was developed by Hallquist based on CAFE method in which semi-discrete equations of fluid and structure had been integrated implicitly while the fluid boundaries had been modeled by DAA methods and plane wave approximation[5]. In 2008, the ABAQUS software appeared in the markets based on the same method, but it is distinct, as the fluid field was modeled based on the method of the boundaries of curved wave approximation [6]. When an explosion occurs in the vicinity of a structure, the assumption of the small motions of the fluid cannot be logical anymore and it is possible to use hydrocodes as referred to in [7]. These hydrocodes have been mentioned along with the method applied for the problem analysis. Recently, in 2002, Sprague and Geers enumerated the disadvantages of CAFE model and proposed a new method based on spectral elements[8]. In spectral elements, the three-line functions used in the finite element CAFE model are removed and replaced with Legendre functions. In fact, it can be said that the accuracy of spectral elements has been integrated with the flexibility of finite elements in CAFE. Moreover, they used the idea of separating the fluid environment into the total field and intervention and diffraction field, in order to express the equations related to the fluid [9,10].
More studies were done by Dyaka, Shin and Li on the non-linear transient response of the submerged circular plates subject to explosion loads [11-13]. In their studies, they used the Kirchhoff theory of thin plates and hypothesized that this plate can show non-linear geometrical and material behavior [11-13]. To analyze the problems of water-structure interaction with the help of numerical methods like finite elements, there are various numerical models such as Lagrangian model, free Lagrangian model (FLM), smoothed particle hydrodynamic model (SPH), total Lagrangian model, Eulerian model, coupled Eulerian-Lagrangian model (CEL) and arbitrary Eulerian-Lagrangian model.

2-1. Theories of water-structure interaction analysis

Normally, in dealing with the issues related to underwater explosions, there are two cases that must be encountered: first explosions close to the free surface, second the areas far from the free surface (ocean depths). The importance of this topic has been increased due to a critical phenomenon called cavitation. This phenomenon which has a completely non-linear nature plays a major role in the analysis of the issues concerned with water-structure interaction.

2-2. the fluid field away from the free surface without cavitation

Thus far, advanced computational methods have originated to deal with underwater shockwaves at the depths of oceans where there is no cavitation. In these models, the fluid is assumed as an infinite and

homogenous acoustic field, while the structure and probably the fluid which is close to the structure are modeled by the finite element method, the impact of fluid field through one of the boundary element, or finite element methods which are engaged in the finite element model of the structure as a system.

2-3. Doubly asymptotic approximation (DAA)

One of the effective methods for the fluid field modeling is the doubly asymptotic approximation. It is used in cases where the presence of cavitation is rare and only the diffracted hydrodynamic sound pressure caused by the fluid-structure interaction is important while the total pressure inside the fluid is of no importance. A formulation of this method from the first rank or DAA is expressed in the below equation [14]:

$$M_f \dot{p}(t) + \rho_f c_f A_f p_s(t) = \rho_f c_f M_f \dot{u}_s^f(t) \quad (1)$$

Where M_f is the fluid mass matrix for the surface of the fluid subject to the structure and A_f is matrix diametrical cross-section which changes the knot pressures into knot force. $\dot{u}_s^f(t)$ is the diffraction rate of fluid particles which is perpendicular to the interface of structures and ρ_f is the diffracted term from the total pressure.

The DAA relation is otherwise called the doubly asymptotic approximation as it shows the limited behavior in high frequencies (initial intervals) and low frequencies (final intervals) of the analysis. For high frequency response, the term $\left|\dot{p}_s(t)\right|$ is considerably greater than term $\left|p_s(t)\right|$ in the above equation. Therefore, the second term in equation 1 is omitted which in turn leads to the plane wave approximation in which $p_s(t) = \rho_f c_f u_s^f(t)$ and is accurate for the short sound wavelengths. However, for low frequency responses, term $\left|p_s(t)\right|$ is considerably greater than term $\left|\dot{p}_s(t)\right|$ and equation 1 is $A_f p_s(t) = M_f \dot{u}_s^f(t)$ which indicates the mass added to the structure that is accurate for the long sound wavelength. The equation of compatibility between the interfaces of the fluid and structure is expressed by the below equation [9]:

$$G^T \dot{u}^m = u_i^f + u_s^f \quad (2)$$

Where i and s indicate the speed of the incident wave and the speed of diffracted fluid particles and $\dot{u}^m$ is the vector of structure particles in the interface of the fluid. G^T is the transpose of the matrix on the interface of the structure and fluid. Equation 2 indicates that the speed of the particles inside the fluid and on the surface of the structure is equal on their overlapping surface. Now, by inserting equation 2 into equation 1, the dynamic equation of the fluid behavior with DAA method from the second rank has also been developed by Geers in which higher terms of scattering pressure have been considered. In total, it can be said that DAA is a very effective and useful approximation method for the modeling of the fluid field with the removal of the finite element modeling for the fluid fields with deep structures and its application in the form of a layer of elements on the structure, so that the impact of cavitation can be ignored. In this state, only the term of hydrodynamic pressure caused by the scattered sound waves can be calculated. In figure 1, the schematic DAA model has been illustrated [14].

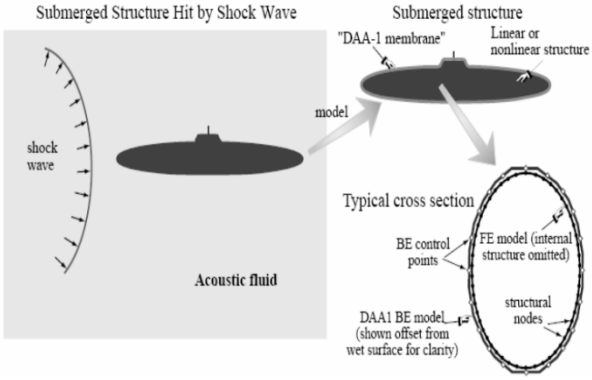

Figure 1. A schematic illustration of the fluid field modeling with DAA boundary element method

2-4. Retarded potential method

This method is indeed an analytical solution for the wave equation (Helmholtz equation). The integrated pressure equation is a function of time, indeed space is discretized by the boundary element method and then the equation has been analyzed with the motion equation of the structure as a system [15].

Suppose a submerged surface is subjected to an incident wave in the water. The fluid field is assumed to be incompressible and non-adhesive. The pressure of the incident wave is expressed as P_{inc} that hits the structure and produces intervention and scattered waves or P_{sca}. Moreover, the responses of the structure also produce a radiation pressure P_{rad} within the fluid field. Therefore, the total pressure consists of three parts as described below [15]:

$$P = P_{inc} + P_{sca} + P_{rad} \quad (3)$$

The boundary terms of the wetted surface of the structure is described as follows equation 4 where n is the normal vector towards the outside from the fluid to the structure, p is fluid density and a_n is the normal velocity of the structure [15]:

$$\frac{\partial P}{\partial \eta} = -\rho a_n \quad (4)$$

In fact, equation 4 shows the active fluid field. The integral of retarded potential is the solution of the linear wave equation exposed to the boundary conditions of the wetted surface of the structure [15]. Then:

$$\nabla^2 P = \frac{1}{c^2}\frac{\partial^2 P}{\partial t^2} \tag{5}$$

The integrated form of equation 5 causes P_{inc} on the wetted surface of the structure subject to the incident pressure wave. This pressure is formulated as follows:

$$R = |x - x'|$$
$$t' = t - \frac{R}{c} \tag{6}$$

Where c indicates the velocity of sound in the water and t' is the delay duration and x is the location of the point where the observations are being performed, and x' is the location of the integrated point.
Equation 6 is the pressure equation in relation to the equation of the structure, the convergence of responses can be achieved by the step-time implicit solutions.

2-5. The field of fluid close to the free surface exposed to cavitation

2-5-1. Acoustic fluid field

The acoustic fluid suggests the behavior of liquid and gas subject to a rapid dispersal such as shockwaves and sound vibrations that spread with the intervals within the range of sound frequencies. The equation of momentum, continuity, and the equation of motion are used to obtain the equations for the expression of acoustic fluid. The classic wave equation for the acoustic fluid in volume V is expressed as below [16].

$$c^2\nabla^2\psi - \ddot{\psi} = 0 \quad in\ V \tag{7}$$

The displacement function ψ is introduced as the quantity of the dependent variable and is defined for the discretization of finite elements as:

$$\psi(x,t) = N(x)\,\psi(t) \tag{8}$$

Where $N(x)$ is the function of the form and $\psi(t)$ is the group value of ψ
This function should satisfy the terms of continuity. Galerkin method is used to obtain the semi-discrete equation of the finite elements. By integrating the wave equation in volume V and based on the function of weight N, we have [16]:

$$\int_V \left[NN^T\ddot{\psi} + c^2(\nabla N)(\nabla N)^T\psi \right] dV = c^2\int_S N\frac{\partial\psi}{\partial n}dS \tag{9}$$

Where T indicates the stimulation that the structure applies on the fluid.
The matrix form of the previous integral is transformed as follows:

$$Q\ddot{\psi} + c^2 H\psi = c^2 b \tag{10}$$

The nature of interaction between the three parts of the engaged system has been shown below in a schematic figure [16]:

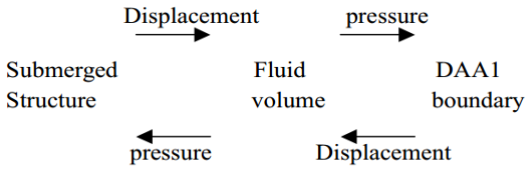

In fact, with the pressure being applied by the fluid volume on the structure, a response in the form of displacement is elicited on the fluid volume and then the fluid receives the pressure from the transfer boundaries and receives it as a displacement quantity again. It is noteworthy that in case there is no cavitation, it is possible to ignore the model of fluid volume and achieve a method called surface approximation methods, in which the structure engages the DAA boundaries or other approximation methods.

2-5-2. Wet surface approximation for problems close to the free surface

In these methods, the fluid-structure interaction has been merely considered based on wet structure surface approximation methods. The motion equation of the structure and DAA equation will be used with the compatible relationship between the particles and the structure for solving the interaction system and the dynamic response of the structure [17].
The equation of asymptotic approximation that is of the first rank is derived as follows [17].

$$M_f\,\dot{p}_s(t) + \rho c A_f\,p_s(t) = \rho c M_f\,\dot{u}_s(t) \tag{11}$$

Where M_f is the matrix of the fluid mass for the wetted surface of the fluid mesh (attached to the structure) and $u_s(t)$ is the velocity vector of fluid particles and vertical particles of the wetted structure surface [17].
Equation 11 is referred to as the doubly asymptotic approximation as it incorporates the system behavior in both of high and low frequencies (or the initial and final intervals) of the responses. The compatibility equation between the fluid and structure is as follows:

$$G^T\dot{x} = u_i + u_s \tag{12}$$

This equation states that the speed of fluid particles and that of the structure elements on the wetted surface of the structure are the same. This means that the particles move together. By insertions in equation 11, one can writes:

$$M_s\ddot{x} + C_s\dot{x} + K_s x = -GA_f\left[p_i(t) - p_s(t)\right]$$
$$M_f\,\dot{p}_s(t) + \rho c A_f\,p_s(t) = \rho c M_f\left[G^T\ddot{x}(t) - \dot{u}_i\right] \tag{13}$$

The above equations are solved for x and p_s values in temporal steps. The promoted DAA method of the second rank is also available. However, the surface approximation methods cannot show the cavitation impacts at the time of shockwave incident on the hull and their reflections and the resulting cavitation beneath the ship [17].

3-validation studies of scalar method principals for structure exposing to under-water explosion waves

3-1. Parametric discussion of tension wave propagation in finite element with explicit dynamic solution

In this section, parametric discussion of principals expressed about explicit dynamic solution and the manner of tension wave propagation in a block under explosive loading are presented considering principals. Parameters such as stability time and the effect of small or large mesh of finite elements and material selection on choosing stable time increment are addressed. As tension waves pass a block with the highest frequency, a very small time increment should be selected for achieving reactions with acceptable accuracy.

3-1-1. Model description

Intended block is made of steel, and its dimensions and load direction is shown in figure 2. In order to study a one-dimensional situation, boundary conditions are selected in such a way that all sides have free movement (roller support). In addition, free end of the block is exposed to an explosive loading with magnitude of 0.1 MPa and continuity time of $3.88 * 10^{-5}$.

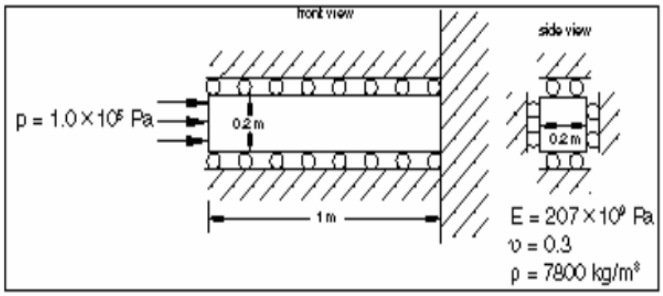

Figure 2. Side view of the model, material characteristics, and load applying method

Wave velocity within the steel can be calculated using material characteristics (ignoring Poisson effect).

$$C_d = \sqrt{\frac{E}{\rho}} = \sqrt{\frac{207\times10^9}{7800}} = 5.15\times10^3\ m/s$$

A wave having this velocity can reach the end of the related block which is 1 meter long after $1.94*10^{-4}$ s. Mesh should be chosen in such a way that it can show the tension passing the block adequately. Bathe proposed that the idea used in finite difference method can be used for cases in which we face wave propagation in an environment to select elements' dimensions and time increment [12]. Mesh dimensions are obtained by selecting 10 elements in each wave length and performing the following simple calculations:

$$L_{10el} = (3.88\times10^{-5})c_d = 0.2$$

The length of 10 elements is 0.2 m and as the length of one element is 1 m, 50 elements are obtained along the block. In addition, 10 elements are also selected in two directions perpendicular on wave propagation. Applied elements are of C3D8R (Eight-node brick element with reduced integration) type (figure 3).

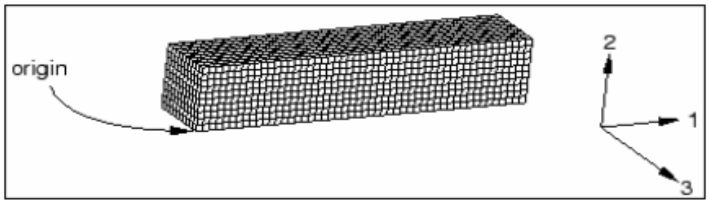

Figure 3. Meshing the block along wave propagation direction and perpendicular on it

3-2. Reaction of submerged shell structure to under-water explosive waves and bed reflection effect

Modeling the reaction of submerged structures with simple geometry to different kinds of under-water explosions is one of the most important parts of validating water and structure interaction codes. In this example, the ability of ABAQUS/Explicit software for modeling the interaction between spherical and cylindrical shell exposed to different shapes of shock waves resulted from under-water explosion, has been investigated. In addition, a parametric study is performed on the shape and type of explosion wave and the structure distance from the bed (reflection boundary). Obtained results are compared with DAA method discussed previously.

Interaction between a spherical and cylindrical elastic hollow shell and shock wave is investigated in planar shapes with time step function, in planar wave with exponential decay and in spherical wave with exponential decay. The magnitude of shock wave in all models is 1 MPa (except cylindrical shell model with step planar wave which is 1 Pa). Explosion resource distance from the reference point on the structure depends on the loading (planar or spherical). Exponential constant time for cylindrical and spherical shell loading is 0.0137^{ms} and 0.685^{ms}, respectively. Figure 4 shows the different types of loading used in this analysis. Symmetry properties are used in these models and suitable boundary condition is used in edges. Cylindrical shell are modeled with S4R elements and its surrounding fluid elements with AC3D8R elements while spherical shell is modeled with SAX1 elements and fluid environment with

ACAX4R for reducing calculation expenses. Spherical and circular non-reflective boundary (radiative) on outer surface of the fluid are considered as infinite boundary for circular and cylindrical shell, respectively. Figure 5(up and down) shows the structure and fluid model. Water and structure interaction will be performed based on the method explained in chapter 4 which is through surface interaction and explicit method during 27^{ms} for the sphere and 6.56^{ms} for the cylinder with time increments of $1*10^{-7}$. Explosion is along positive axis 2 for the sphere. The closest point to the explosion area is called the leading node and the farthest at the back of the sphere is called the trailing node in figure 5. The leading point is a place where shock wave reaches it at the first moment and it is also called the standoff point. As it can be observed, the radiative boundaries are also placed at the outer surface of the fluid. Properties of material used for the fluid and the structure based on Huang sphere [13, 14] are as follows:

Steel properties:

$$Radius\ of\ \ sphere = 1^{m}\ ,\ \rho_s = 7766\,{kg}/{m^3}$$

$$Radius\ of\ \ cylinder = 1^{m}$$

$$\nu = 0.3\ ,\ t_{sphere} = 2^{cm}\ ,\ t_{cylinder} = 2.9^{cm}$$

Fluid properties:

$$\rho_f = 997\,{kg}/{m^3}\ ,\ c = 1416\,{m}/{s}\ ,\ K_f = 2.128\times10^{9}\,Pa$$

Outer boundary radius for spherical shell=3 m

Outer boundary radius for cylindrical shell=2.03m

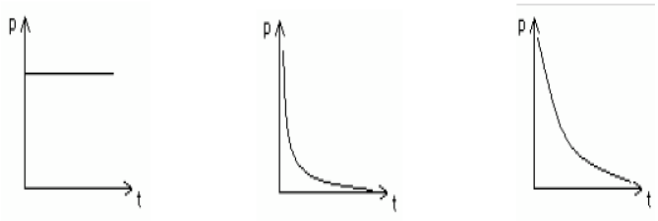

(I) (II) (III)

Figure 4. . different loading type used in this analysis: I) step incident load; II) shock wave with time constant of 0.0137 ms; III) shock wave with time constant of 0.685 ms

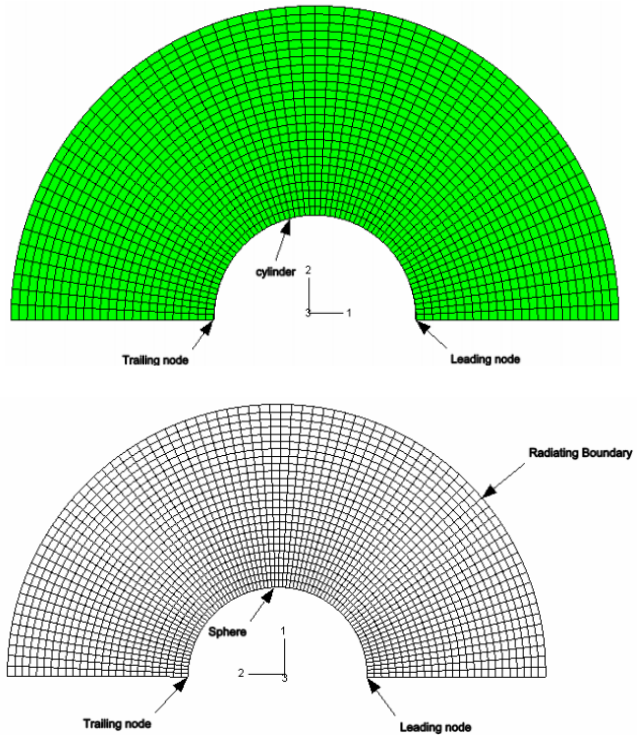

Figure 5. a view of symmetrical model with its surrounding fluid; Up) spherical shell in which explosion occurs along axis 2; Down) cylindrical shell in which explosion occurs along axis1

3-2-1. Studying pressure variations inside the fluid

In order to study this model and pressure variation in the fluid during the analysis more carefully, total pressure variations is shown in figure 6 for 0.006^{s} time increment. As it is observed, reflected wave reaches the structure after 0.003^{s}. Total pressure variations inside the fluid are plotted using total wave option. Pipe transformation is plotted in figure 7 from the analysis start until the end of it for 0.001^{s} time increment. As it can be seen in the following figures 8, when shock wave reaches the first point, i.e. standoff point, this point of the cylinder starts to transform. Reflected wave strikes the structure after 0.003^{s} and the cylinder starts moving perpendicularly.

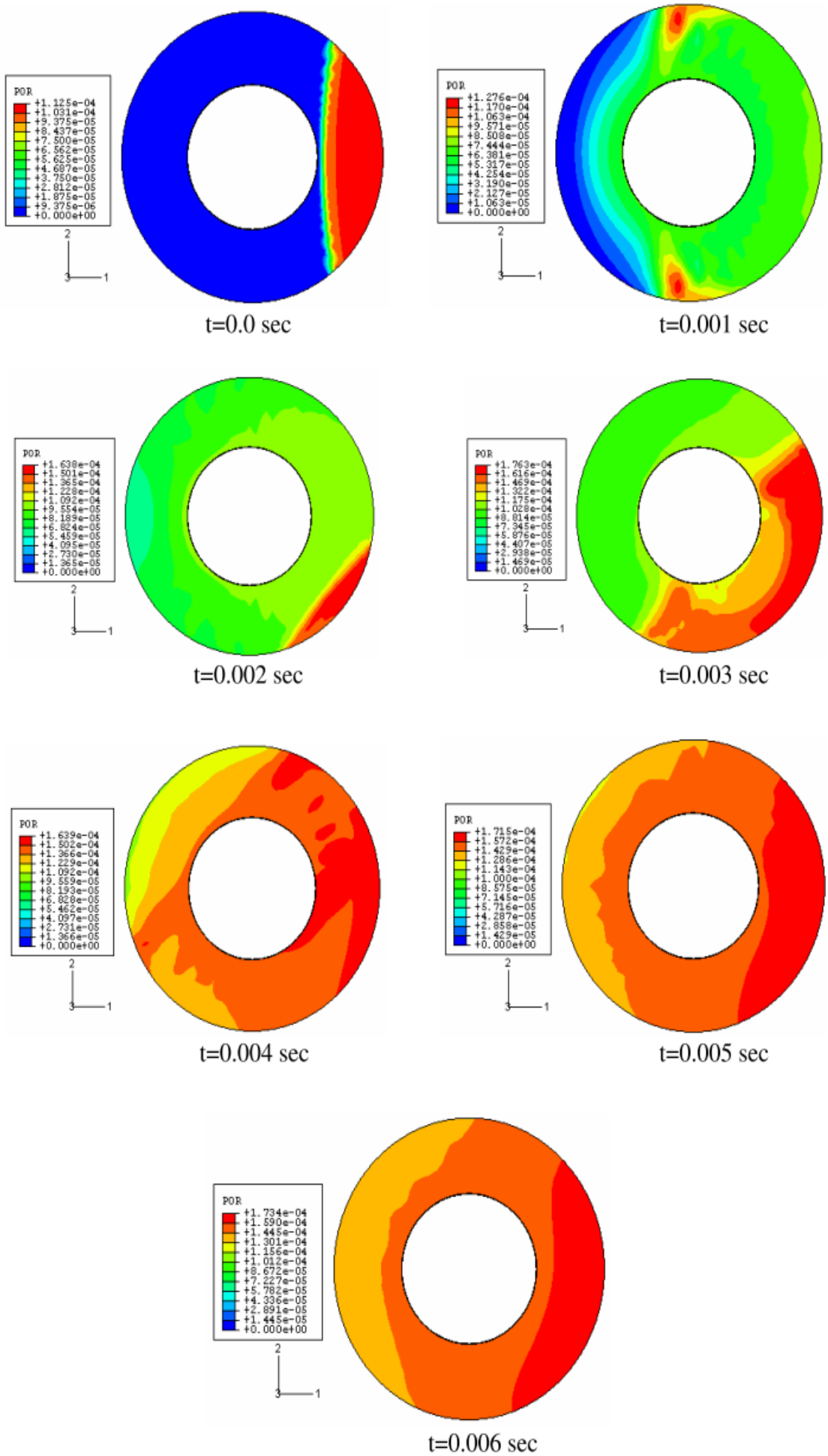

Figure 6. Total pressure variations in fluid field in Pas and based on 0.001-s time increment in scale 1*10-9

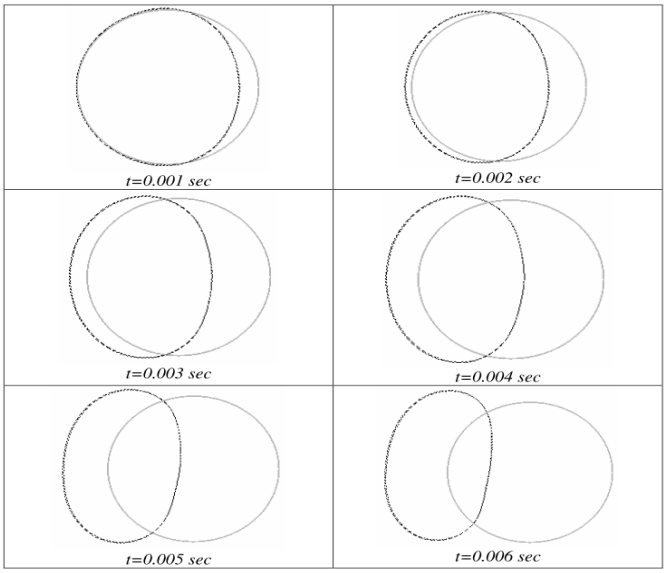

Figure 7. cylinder movement due to direct and bed-reflected waves from the beginning till the end of analysis with 0.001-s time increment

It can be generally said that bed reflection leads to reaction increase. This is because incident wave and reflected wave have the same sign. In order to better understand the results, cylinder transformation in the last time increment is plotted in figure 10 for different magnitudes of incident wave.

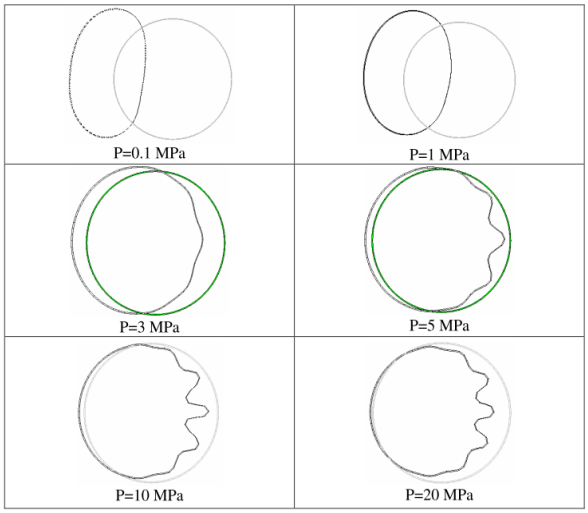

Figure 8. Cylinder transformation regarding the magnitude variations of incident wave at moment 0.006 s in scale 1000

It is better to study total pressure variations in fluid field in order to understand the procedure happened in this study. These variations are shown in figure 9. As it can be observed, when analysis and forward movement of the cylinder progress, points near the explosion resource face intense hydrodynamic pressure variation. In so far as some points one the cylinder receive very high pressure while the adjacent point on the structure and the surface opposite the explosion experience very low pressure. This pressure difference is due to the effect of the wave reflected from the bed which leads to transformation shown in figure 8.

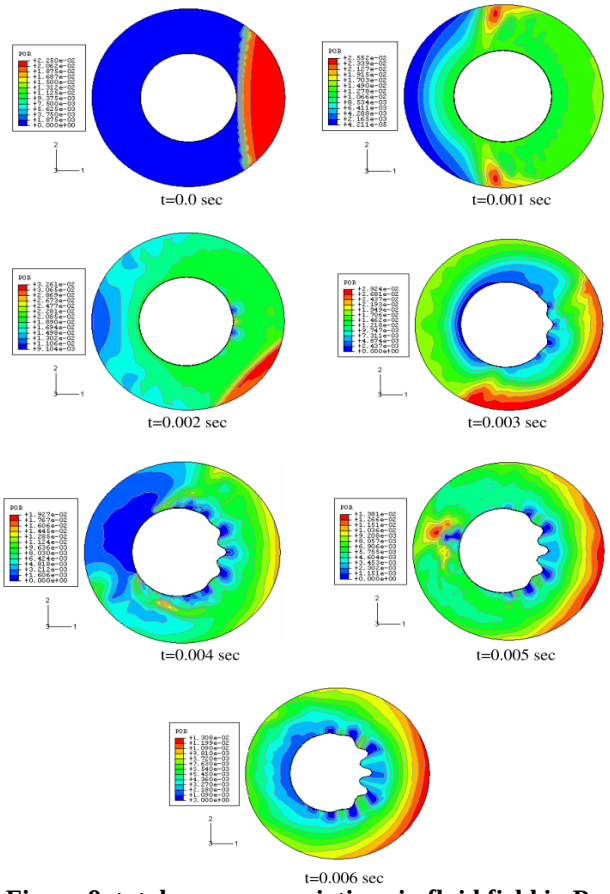

Figure 9. total pressure variations in fluid field in Pa and based on 0.001-s time increment and in scale 1*10^{-9}

4- Problem statement and explaining its geometry

In this example, the shock wave created by 60 lb explosives HBX-1 (equivalent to 20.17 Kg TNT) is generated. The material of the cylinder was aluminum T6061-6. The characteristics of the materials used for water and the structure are as follows:

Aluminum characteristic:

$$\rho = 2784.5\,{kg}/{m^3}\ ,\ E = 7.56\times10^{10}\,Pa\ ,\ \nu = 0.33$$

$$Plasticity\ data\begin{cases} Yield\ Stress = & 3.0E+8Pa & 3.3E+8Pa \\ Plastic\ Strain = & 0.0 & 1 \end{cases}$$

Water characteristics:

$$\rho = 1000\,{kg}/{m^3}\ ,\ K_f = 2.1404\times10^{10}\,Pa\ ,\ c_f = 1463\,{m}/{s}$$

Geometry characteristics of the pipe and the shock wave are mentioned in the table 2.

Table 2. the cylinder's geometry characteristics and the magnificence of the shock wave

Length (m)	External diameter (m)	The thickness of the pipe wall (mm)	Distance to the free area (m)	The thickness of the end lid (mm)	The distance of the explosion source to the structure (m)	Shock wave magnificence MPa
1.067	0.303	6.35	3.66	25.4	7.62	15.7

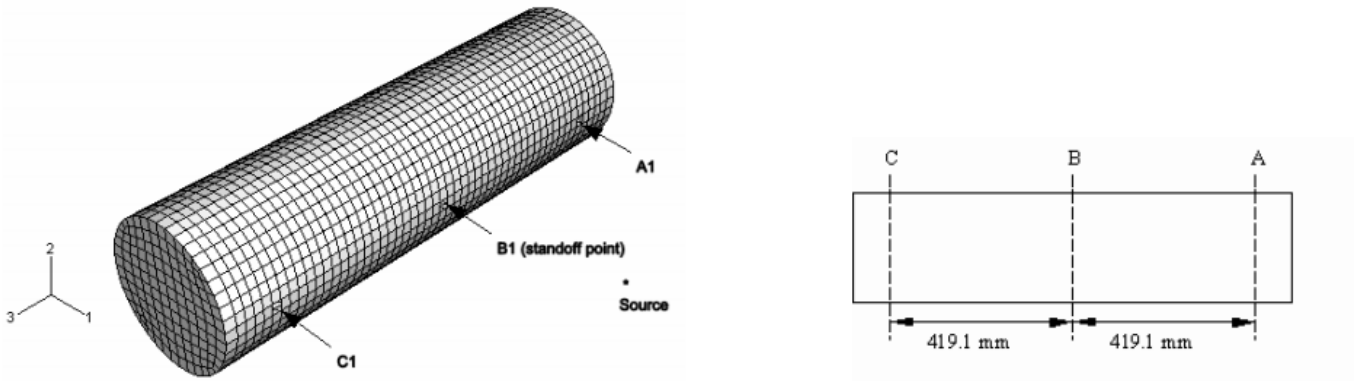

Figure 10. The site of displacement of the strain gauges, explosion source, and the reference point on the immersed pipe

The cylinder is placed horizontally at a depth of 3.66 m from a pool with a depth of 40 m. The explosive is also located at an identical depth perpendicular to the cylinder axis on its' center at a distance of 7.62 m of the external area of the cylinder. The depth of the location of the cylinder, the place of explosion and the time of experiment is in such a way that the cavitation effect, the gas bulb, the reflection from the walls, and the free area can be ignored (the assumption of lack of cavitation will be investigated). Strain gauges are placed at different positions from the external area of the cylinder (Figure 10) .The shock wave exerted is spherical which is shown in figure11. The magnificence of the shock wave is 15.7 MPa.

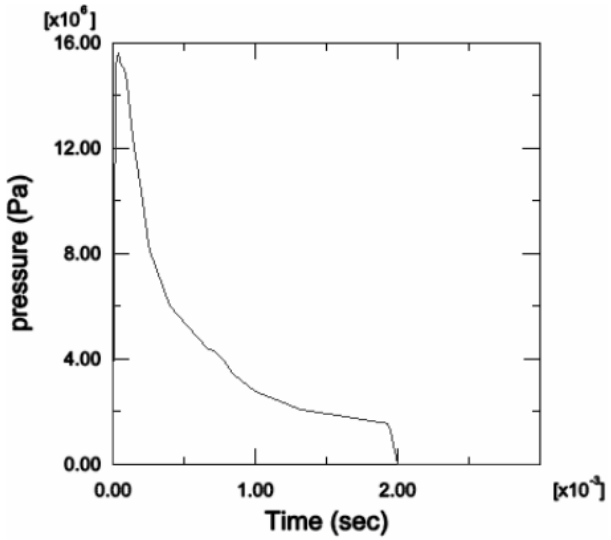

Figure 11. The graph of the wave induced by the explosion under the water at a distance of 7.62 meters from the explosion source

To model the cylinder, shell elements S4R of limited components have been used. This meshing includes 2402 nodes and 2400 elements with 40 contextual divisions and 53 axial divisions, in such a way that the dimension of each element is almost 2 centimeters. The normal vector of the elements is towards the fluid. Nodes are places on the external area of the shell. End lids are dummy elements which are used with decreased mass and stiffness, and only indicate the thickness of the lids.

The external fluid is modeled by elements of the AC3D8R four dimensional model. External boundaries of the Radiating boundary condition (Nonreflecting) of the fluid has been modeled by two cylindrical and spherical parts. On the basis of the equations given in chapter four for the calculation of the distance of reflective boundaries, this value is obtained equal to 0.457 m, but according to the conducted studies, here to reduce the effects of the added mass on the first bending mood of the structure for lower frequencies, twice its value brings upon a better result [15]. Therefore, a study was conducted on the basis of the varying distances of the two infinite cylinders between which is filled with water, to determine the ratio of the added mass at the lowest bending mood of the structure. The results are presented in table3. As it can be seen, in a radius, 6 times as the internal radius of the cylinder, the percent of error induced by added mass to the first bending structure is 5.7% relative to the infinite boundaries. On the other hand, Belvin conducted a parametric analysis on the basis of the ratio of the external infinite cylinder radius to the internal infinite cylinder radius whose context was filled with water, to determine the error induced by the effect of the added mass of the fluid on the structure. His results showed that for the external cylinder radius in the limit of 6 times as the internal cylinder radius, the error of the ratio of the added mass to the first bending mood of the structure is almost 6 percent relative to the infinite boundaries [16]. This result is consistent with the result obtained here. Therefore, for the distance of reflective boundaries to the model center, the value of 0.915 meter is used. To mesh the fluid in contact with the structure, the seeding of 0.04 m with the division of 24.4 elements in each sound wavelength with a frequency of 1500 Hz, and in the boundary part, the thicker seeding whose seeding is 0.1 m, i.e. 9.7 element in each sound wavelength with a frequency of 1500 Hz is used. This characteristic leads to reduced calculation costs

The system involved between the fluid and the structure in this example is between the hydrodynamic pressures induced by the sound waves which is

present in the fluid, and displacements of the cylinder in their contact. Here, the surface intra-action solution method has been used. Because the fluid mesh is thicker, the fluid area is considered as the Master and the structure area is considered as the slave.

Table 3. the ratio of the mass added to the structure in the effect of variations of external boundary radius

Cylinder Radius Ratio (R_0/R_i)	Added Mass Ratio (External boundary/Infinite Domain)
1.5	2.500
2.0	1.665
4.0	1.141
6.0	1.059
8.0	1.031
16.0	1.007
24.0	1.002

5-Results

The analysis occurs at 0.008 seconds (similar to laboratory conditions) by explicit method. The stable time step is calculated 1.69×10^{-6} for critical elements in pre-processing point. In the first part of results, the general condition of the case such as reasonable amount of kinetic energy and strain energy and the amount of plastic energy and the total amount of energy will be discussed using the internal energy of structures charts. Fig. 12 indicates that as soon as the shock wave loading finishes and the pipe begins vibrate while the kinetic energy ALLKE increases, at the same time the strain energy ALLSE is beginning to decrease. When the pipe is at its maximum deformation, the maximum amount of strain energy occurs, while in other times when the pipe is vibrating, the strain energy is at its minimum. Considering that ALLPD plastic strain energy is reaching to a stable situation, then it increases after a while. It is shown from the kinetic energy plot that the second bulge in the amount of plastic strain energy occurs when the pipe is returning from its maximum deformation. Therefore, the plastic deformation after shock wave loading can be observed. In ABAQUS, the element's hour-glassing deformations are controlled by the ALLAE quantity, virtual strain energy. It is shown that as the internal energy dissipates and plastic deformations of the pipe form according to structure's deformations, the amount of total internal energy itself is much higher than the amount of elastic strain energy. Therefore it is concluded that the virtual strain energy in this analysis is an energy quantum including the dissipated energy with elastic strain energy. ALLIE is the total internal strain energy including all internal energy quantities (ALLSE+ALPD+ALLAE). It is shown in Fig. 12 that the virtual strain energy is approximately 1% of the total energy. It shows that in this analysis, the hour-glassing deformations are negligible [17].

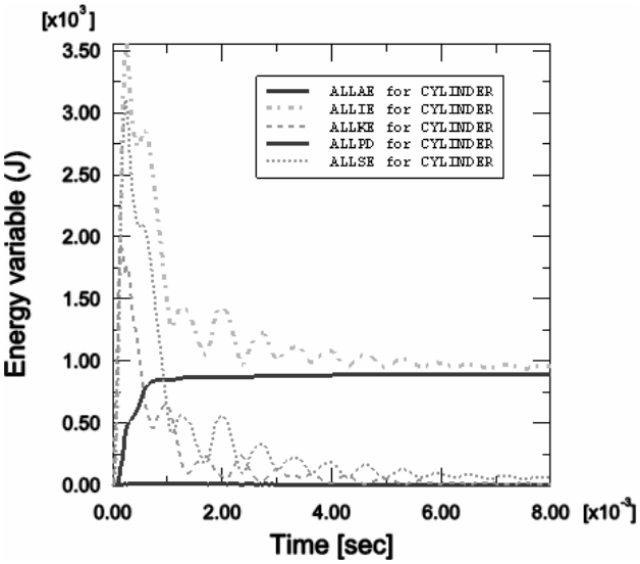

Figure 12. Comparison of the structure's internal energy and kinetic energy

As it is shown in the free vibration mode, the upper and lower points moving in opposite directions. In Fig. 13 this mode plotted on the scale of 40.

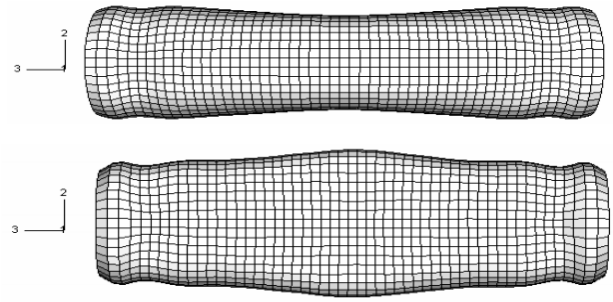

Figure 13. Breathing mode of plunged pipe in two different moment of analysis on the scale of 40

Another movement of the pipe is in 1 axial, actually two surfaces in front of and behind the explosion move towards the shock wave propagation. In Fig. 14 the deformation of this mode is plotted in two different times on the scale of 20.

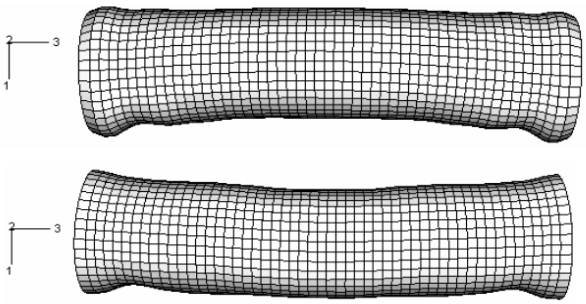

Figure 14. The whipping mode of plunged pipe in two different times on the scale of 20.

The tension obtained from ABAQUS analysis for two surfaces behind and in front of the explosion after 0.008 seconds and plotted in figures 15 and 16. As it has been represented, after a while the tension near the end crust of the pipe increases. As mentioned before, this happens because of the pipe's two ends thickness.

This can be observed in strain charts. The strain value is higher in A1, B1 and C1 strain gauges. The tension at the last moment of analysis for B1 obtained 145 MPa. Although the tension in this point is 272 Mpa, the accumulated equal plastic strain counter OEEQ is plotted in figures 17 and 18. It is shown that the accumulation of strain at the end of the pipe causes plastic deformation in this region.

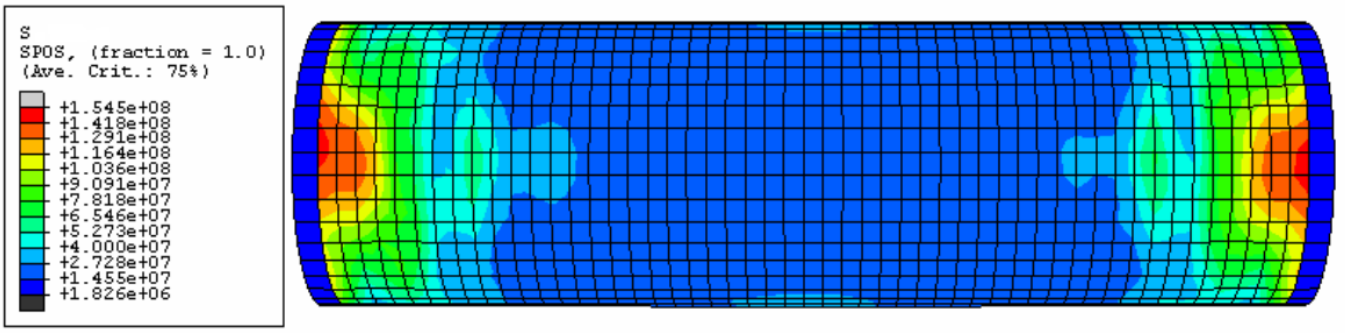

Figure 15. Tension counter on the front surface of explosion at 0.008 seconds.

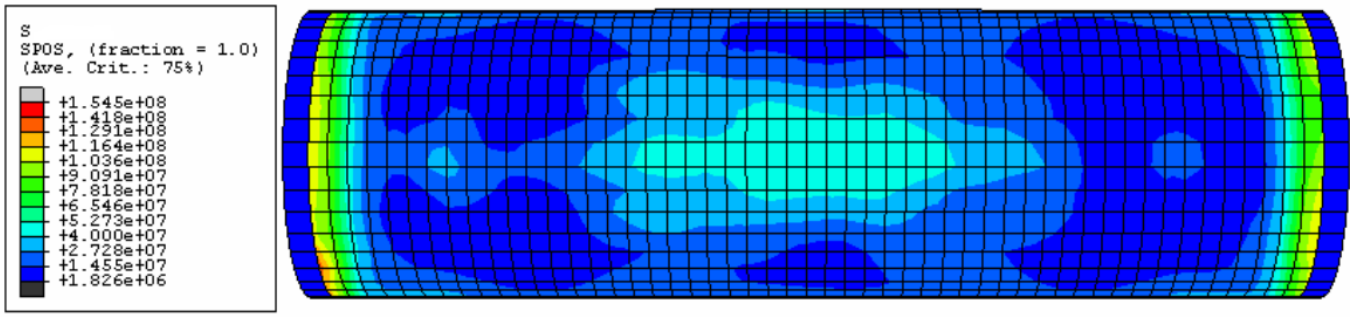

Figure 16. Tension counter on the back surface of explosion at 0.008 seconds.

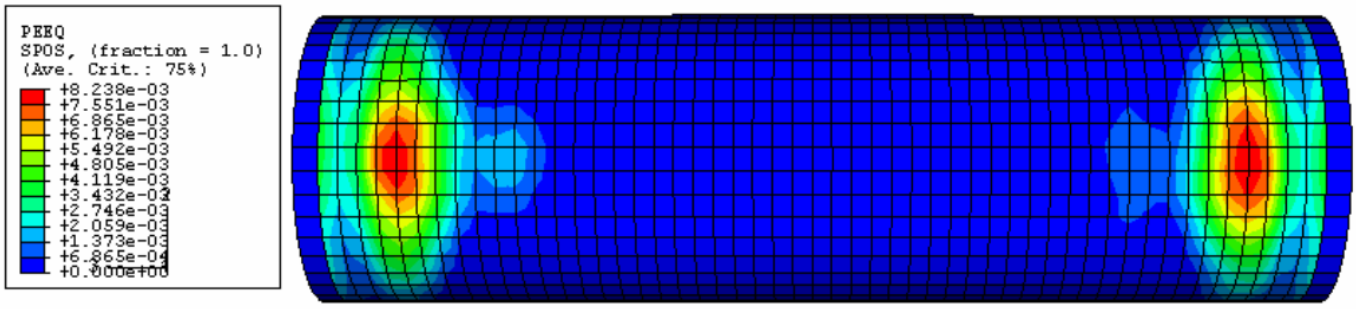

Figure 17. accumulated equal plastic strain counter on the front surface of explosion at 0.008 seconds

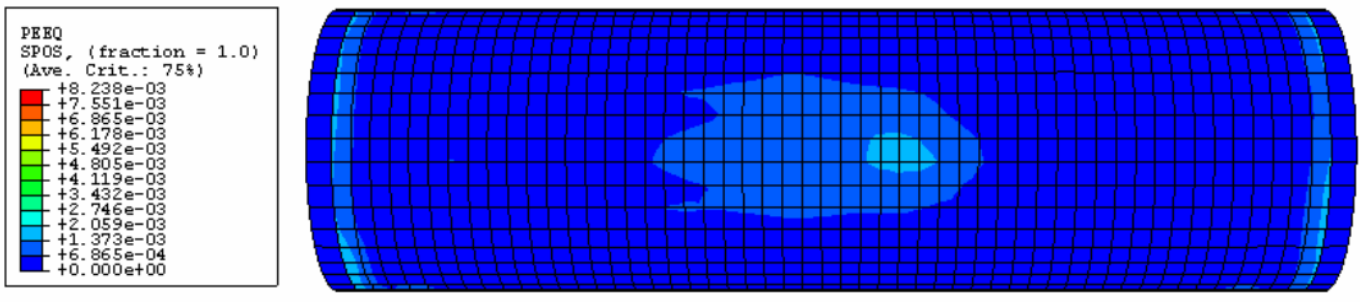

Figure 18. Accumulated equal plastic strain counter on the back surface of explosion at 0.008 seconds

As said before the cavitation created in this region is like a protection layer against shock wave harsh effects. Therefore, it can be pointed that cavitation is the cause of decreasing the strain in this point. Fig. 19 indicates the deformation at 0.008 seconds. It is shown that deformation at the end is lower than the middle parts of the pipe. Fig. 20 and Fig 21 indicate total hydrostatic pressure caused by shock wave interaction with plunged pipe from the beginning to the end of the analysis.

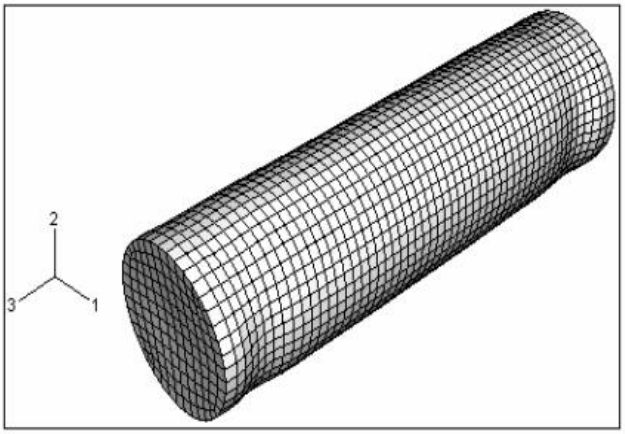

Figure 19. . Deformation of the pipe at 0.008 seconds on the scale of 20.

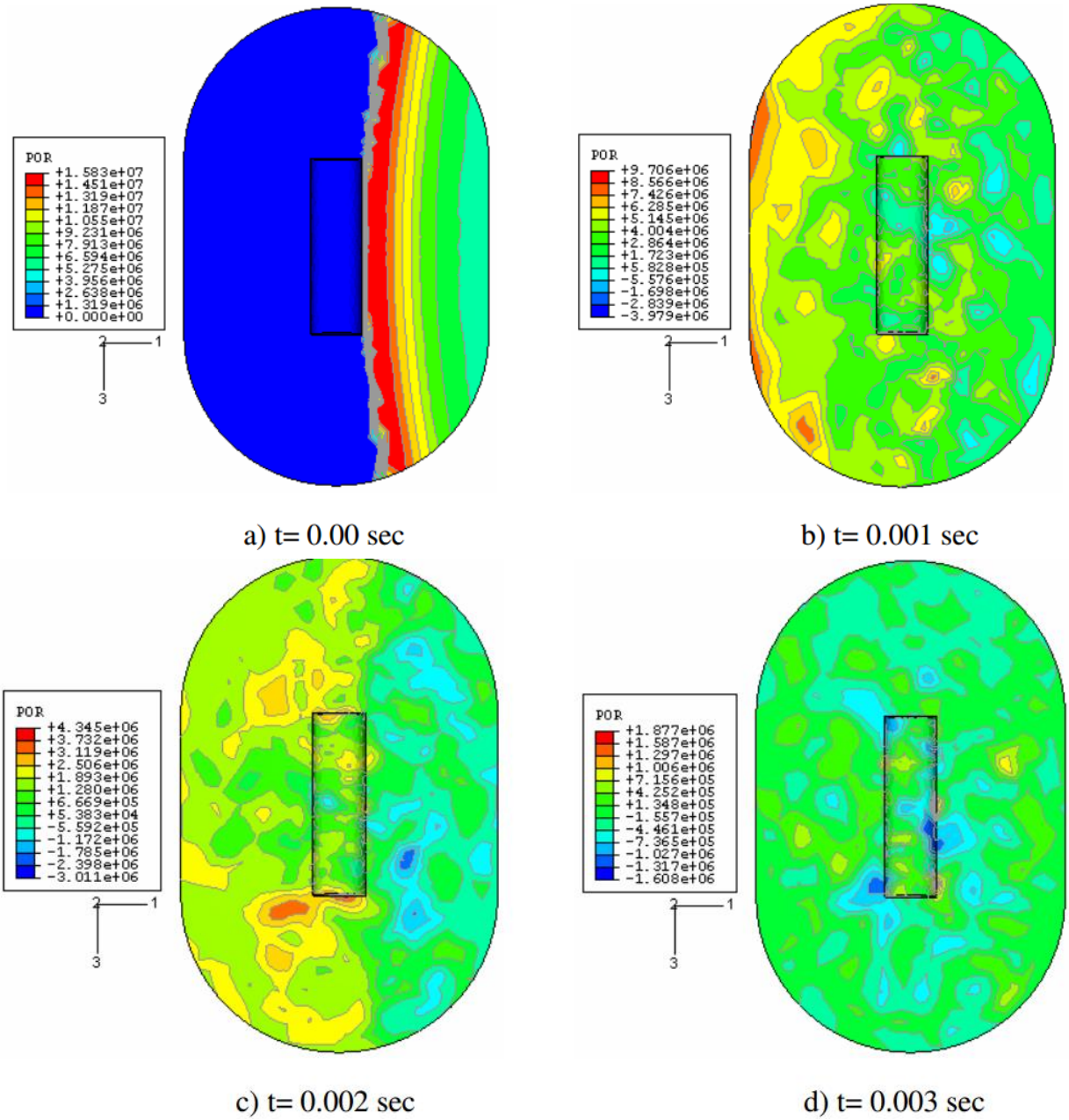

Figure 20. Total hydrostatic pressure caused by shock wave interaction with plunged pipe from the beginning to the end of the analysis.

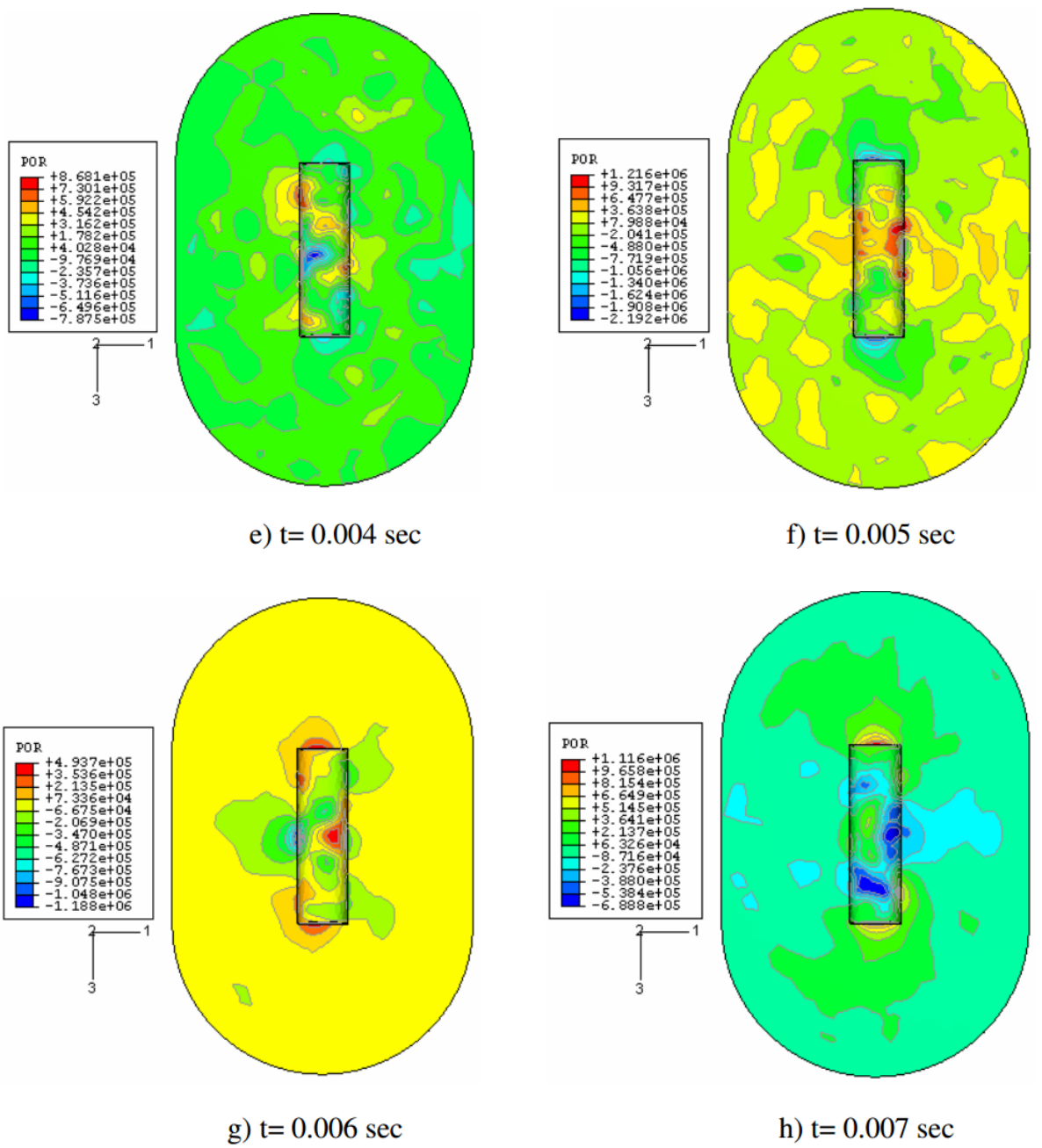

e) t= 0.004 sec f) t= 0.005 sec

g) t= 0.006 sec h) t= 0.007 sec

Figure 21. Total hydrostatic pressure caused by shock wave interaction with plunged pipe from the beginning to the end of the analysis.

6-Conclusion

As it is noted in the topic of underwater explosion, water and construction interaction derived from, explosive waves which we are dealing with different issues such as a dynamic equation selection method governed fluid particles movement, reasonable hypothesizes about them and the function field of these equations, different boundary conditions such as radiation boundaries, reflective boundaries and interaction boundaries, selecting a proper solution method for the system involved with water and construction after explosion and selecting a proper solution method for time step and dimension of usable elements, the pulses derived from gas bubbles model and so on. The following results are obtained for some of the above factors in this research, after the related modeling. As the result of analyze, it could be mentioned that in this level of issues where the system totally is involved between the construction movements and the sound pressure, the construction responses are according to the following:

The response with low frequencies is recognized by construction wavelengths which basically are significantly smaller than the sound wavelengths. In this situation, the effect of the external fluid is as an added mass upon the wet surface of the construction. The high frequency response is recognized by the construction wavelengths which basically are significantly bigger than the sound wavelengths. In this situation, the effect of the external fluid is as a simple damping mechanism, so that the energy from the construction to radiative bound (zone) is transferred by sound hydrodynamic waves. The medium frequency response is recognized by the

construction wavelengths which are equal with the sound wavelengths. During this frequency diet the external fluid is acting under two effects, the added mass and the damping effect upon the construction.
Determining the place of radiation boundary in interaction of water and construction derived from underwater explosion is very important, because it should be able to show the highest created wavelength adapted to the lowest frequency governed on fluid field. As it mentioned in these frequency values, the fluid is acting as the added mass on the construction. So the radiation boundaries must be in a position where it shows the minimum error from fluid added mass on first flexural mode. A parametric study upon a pipe float showed that at distance about 7 times of internal cylinder's radius, radiation boundaries had the minimum effect of added mass on first flexural mode. Also the research showed that in reflective boundary conditions, reflected waves from the seabed causes the increasing of responses, however the waves which are reflected from the surface of sea causes the reduction of responses. This effect with a time difference in construction responses is due to more distance which the reflected wave moves to arrive to the construction surface from fluid field external surfaces. Moreover, a parametric study on shock wave amplitude changes represented that some parts of construction around the explosive supply are affected by hydrodynamic pressure extreme changes. This factor creates irregular deformations in this surface of pipe. According to parametric studies, it is represented that plane waves is creating a stronger effect with the time step function. Also in this kind of loading, construction response in final seconds of analyze does not fluctuate between zero amount, against loading by reduction exponential time function. As it was noted in Kwon and Fox cylinder modeling when the shock waves arrive to the float construction, the area of pipe near the explosive supply in primary seconds is involved cavitation. It is the effect which was not paid attention in previous researches. So the hypothesis, the cavitation area can act as a protective layer for the construction against shock waves. The obtained results for near and far strain gauges from explosive area upon the construction, represents the accuracy of the claim. Moreover, this result suggests that DAA method is not applicable enough for areas with high probability of cavitation.

7- References

1- Cole, R. H. (1965). *Underwater explosions. Dover Publications.*

2- Mair, H. U. (1999). *Benchmarks for submerged structure response to underwater explosions. Shock and Vibration*, 6(4), 169-181.

3- Felippa, C. A., & DeRuntz, J. A. (1984). *Finite element analysis of shock-induced hull cavitation*. Computer Methods in Applied Mechanics and Engineering, 44(3), 297-337.

4- Geers, T. L., & Hunter, K. S. (2002). *An integrated wave-effects model for an underwater explosion bubble.* The Journal of the Acoustical Society of America, 111(4), 1584-1601.

5- Zhang, Z., Wang, L., & Silberschmidt, V. V. (2017). *Damage response of steel plate to underwater explosion: Effect of shaped charge liner*. International Journal of Impact Engineering, 103, 38-49..

6- ABAQUS, Users' *Manual, and Theoretical Manual*. "version 6.7, ABAQUS." (2008).

7- Felippa, C. A., & DeRuntz, J. A. (1991). *Acoustic fluid volume modeling by the displacement potential formulation, with emphasis* on the wedge element. Computers & structures, 41(4), 669-686.

8- Sprague, M. A. (2002). *Advanced computational techniques for the analysis of 3-D fluid-structure interaction with cavitation*(Doctoral dissertation, University of Colorado).

9- Jiang, J., & Olson, M. D. (1996). *Non-linear transient analysis of submerged circular plates subjected to underwater explosions.* Computer methods in applied mechanics and engineering, 134(1-2), 163-179.

10- Geers, T. L. (1978). *Doubly asymptotic approximations for transient motions of submerged structures.* The Journal of the Acoustical Society of America, 64(5), 1500-1508.

11- Dyka, C. T., & Ingel, R. P. (1998). *Transient fluid-structure interaction in naval applications using the retarded potential method*. Engineering analysis with boundary elements, 21(3), 245-251.

12- Shin, Y. S. (2004). *Ship shock modeling and simulation for far-field underwater explosion.* Computers & Structures, 82(23-26), 2211-2219.

13- Li, S., Li, X., Wang, Z., Wu, G., Lu, G., & Zhao, L. (2016). *Finite element analysis of sandwich panels with stepwise graded aluminum honeycomb cores under blast loading. Composites* Part A: Applied Science and Manufacturing, 80, 1-12.

14- Huang, H. (1969). *Transient interaction of plane acoustic waves with a spherical elastic shell.* The Journal of the Acoustical Society of America, 45(3), 661-670.

15- Zhang, W., & Jiang, W. (2017). *Research on the shock resistance optimal design of small-sized submerged vehicle subjected to non-contact underwater explosion.* Proceedings of the Institution of Mechanical Engineers, Part M: Journal of Engineering for the Maritime Environment,

16- Blevins, R. D. (1979). *Formulas for Natural Frequencies and Mode Shapes*, Robert E.

17- Reismann, H., & Pawlik, P. S. (1991). E*lasticity, theory and applications*. Krieger Publishing Company.